Life Cycle Impact Assessment of Iron Oxide (Fe_3O_4/γ-Fe_2O_3) Nanoparticle Synthesis Routes

Asifur Rahman[1], Seju Kang[1], Sean McGinnis[2,3], Peter J. Vikesland[1,2,*]

[1]Department of Civil and Environmental Engineering, Virginia Tech, Blacksburg, Virginia, USA

[2]Virginia Tech Global Change Center and Virginia Tech Institute of Critical Technology and Applied Science, Virginia Tech, Blacksburg, Virginia, USA

[3]Department of Material Science and Engineering, Virginia Tech, Blacksburg, Virginia, USA

***** *Corresponding author*. Tel.: +1; fax: +; E-mail address: pvikes@vt.edu (P. Vikesland).

Postal address: 420 Durham, Virginia Tech, Blacksburg 24061, VA, USA

Abstract

The synthesis of superparamagnetic iron oxide nanoparticles (FeO_x-NPs) has rapidly developed over the past decade due to their wide-ranging applications in research and technology. However, at present there exists very limited knowledge about the environmental impacts of the various input materials and the energy required for different FeO_x-NP synthesis approaches. In this study, we used cradle-to-gate life cycle assessment (LCA) to analyze and compare the environmental impacts of FeO_x-NPs produced via seven common synthesis routes. Four different functional units (i.e., mass, mean particle size, specific surface area, and saturation magnetization) were used to normalize the environmental impacts and evaluate the corresponding changes. Overall, physical and biological synthesis routes exhibited high environmental impacts due to their higher input material and energy requirements. Interestingly, biological syntheses had the highest environmental impacts due to their reliance on bacterial culture media. All of the chemical synthesis routes had lower environmental impacts except the thermal decomposition method, which had higher environmental impacts due its use of non-polar organic solvents during synthesis. The lab-scale LCA inventory data and analysis presented here addresses the existing data gaps and helps guide future research for FeO_x-NP synthesis under industrial conditions. The information generated by this effort aids in the identification of environmentally friendly and sustainable production pathways for FeO_x-NPs.

TOC Art

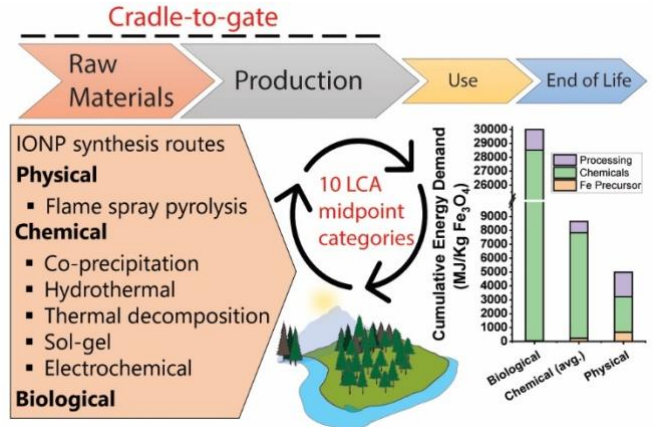
Cradle-to-gate
Raw Materials
Production
Use
End of Life
IONP synthesis routes
Physical
▪ Flame spray pyrolysis
Chemical
▪ Co-precipitation
▪ Hydrothermal
▪ Thermal decomposition
▪ Sol-gel
▪ Electrochemical
Biological
10 LCA midpoint categories
Cumulative Energy Demand (MJ/Kg Fe3O4)
Processing
Chemicals
Fe Precursor
Biological
Chemical (avg.)
Physical

Introduction

Superparamagnetic iron oxide (Fe_3O_4/γ-Fe_2O_3) nanoparticles are a widely used class of NPs due to their controllable size and shape, tunable magnetic properties and biocompatibility.[1, 2] Iron oxide nanoparticles (FeO_x-NPs) have wide ranging applications in biomedical engineering, biomedicine, bio-sensing, energy, electronics, water treatment and environmental remediation.[2-9] FeO_x-NPs had an estimated market value of ≈60 million USD in 2020 that is expected to increase to 87.4 million USD by 2025.[10] Due to the large scale production and widespread use of FeO_x-NPs, research into their potential environmental implications has become necessary to ensure sustainable nanotechnology.

Compared to the rapid growth of FeO_x-NP production and application techniques the evaluation of their environmental impact remains limited. Because FeO_x-NPs have a broad range of applications, several FeO_x-NP synthesis techniques using chemical, physical and biological approaches have been reported in the literature.[3, 11, 12] Co-precipitation, hydrothermal, thermal decomposition, and sol-gel are among the conventional wet chemistry production methods of FeO_x-NPs.[13-16] Flame spray pyrolysis (FSP) is a vapor phase method for large-scale synthesis of FeO_x-NPs, while electrochemical methods have been explored as promising alternatives due to the speed of the process and decreased energy requirements.[17, 18] The use of energy intensive chemicals and reagents in mainstream synthesis methods have recently prompted investigations into alternative 'green' synthesis methods for FeO_x-NPs. Previously, biopolymers were used as reducing and stabilizing agents instead of commonly used organic amines and acids in hydrothermal synthesis of FeO_x-NPs.[19] Plant extracts have been investigated as reducing agents for green synthesis and application of FeO_x-NPs.[20, 21] Furthermore, biological synthesis methods have been developed using bacterial culture as potentially eco-friendly methods of FeO_x-NP production. Recently, the progress in large scale fermentation techniques using continuous fed-

batch culture has allowed scaled up production of biomineralized magnetite/maghemite (Fe_3O_4/γ-Fe_2O_3), also known as 'magnetosomes'.[22]

Life cycle assessment (LCA) can be used to determine the environmental impacts of all the life cycle stages of a product, from raw material to end of life.[23, 24] Previous studies suggest that LCAs effectively quantify the environmental impacts of energy intensive NP production processes.[25-28] LCAs of FeO_x-NP production processes can identify potentially energy intensive components with adverse environmental and health effects. Previously, the environmental impacts of Ag and TiO_2 NPs produced via physical, chemical and bio-based production processes were studied using LCA.[26, 27] Results from these studies showed that impacts associated with upstream production of bulk Ag and Ti were dominant across synthesis routes. Overall, physical and biological routes showed higher impacts compared to the chemical routes. However, there have been very limited studies on the LCA of FeO_x-NP syntheses. Feijoo et al. compared FeO_x-NPs with three different surface coatings (polyethylenimine, oleic acid, SiO_2) via LCA.[29] However, the FeO_x-NPs were exclusively synthesized via co-precipitation with no other synthesis methods examined.[29] Marimón-Bolívar et al. reported the 'green' synthesis of FeO_x-NPs using glutathione as a stabilizer and used LCA to compare its environmental impacts with that of FeO_x-NPs produced via co-precipitation.[30]

The wide range of applications and high reactivity of FeO_x-NPs have prompted investigations into the environmental toxicity of iron oxide nano-waste.[31-33] Workers and consumers can be exposed to FeO_x-NPs in different stages of the FeO_x-NP life cycle, from production to disposal and reuse. During their life cycle, FeO_x-NPs and nano-waste can get into the atmosphere and the aquatic environment through a number of exposure pathways (**Figure 1**). The different chemicals and energy processes required for FeO_x-NP production processes can act

as potential drivers of overall impacts. The availability of reliable and validated inventory data is very limited for FeO_x-NPs, which makes it challenging to quantify the environmental impacts of FeO_x-NP production processes. Such information, if available, could contribute to the improvement of existing synthesis routes and the potential development of novel synthesis routes for commercial scale production of FeO_x-NPs.

In this study, we compiled LCA inventory data and compared the environmental impacts of seven mainstream and lab-scale FeO_x-NP synthesis methods across ten environmental midpoint categories. Four different functional units: mass, mean particle size, specific surface area, and saturation magnetization were used to normalize the data for comparison of the synthesis routes. In addition, the environmental impacts of producing 1 kg of six different Fe precursors were compared using LCA. The cumulative energy demand (megajoules, MJ) to produce 1 kg of FeO_x-NPs by each synthesis route and the different Fe precursors was calculated as absolute indicators of potential environmental impacts. The synthesis methods were evaluated for sensitivity to their dominant synthesis components.

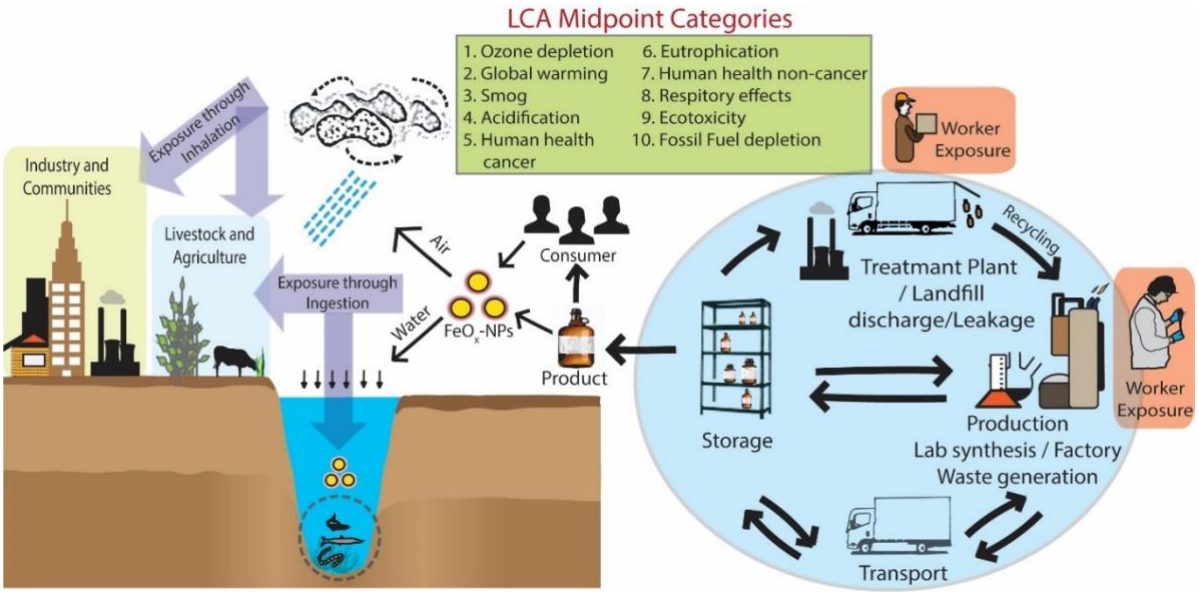

Figure 1. LCA midpoint categories selected based on the common exposure pathways of NPs in the environment.

Methods and Modeling

Following the guidelines suggested by the International Organization for Standardization (ISO), the LCA modeling steps discussed herein consists of: 1) Scope and overview, 2) life cycle inventory (LCI) analysis, 3) life cycle impact assessment (LCIA), and 4) interpretation.

Scope and Overview

This study evaluated the environmental impacts of seven mainstream synthesis methods of FeO_x-NPs, as well as six different Fe precursors based on their 'cradle to gate' (from raw materials to production) LCA profiles. The materials and input energy requirements for the FeO_x-NP synthesis methods and Fe precursors were obtained from the literature on lab-scale synthesis methods of FeO_x-NPs. Furthermore, energy intensive reagents and processes were identified and their contributions to the overall environmental impacts were quantified for each synthesis method.

Life Cycle Inventory (LCI) Analysis

Synthesis Procedures

A summary of the synthesis methods studied are provided in **Table 1.** Details of the procedures and reaction mechanisms for the Fe precursors and synthesis methods are provided in the **Supporting Information (SI)**. To construct the inventory for each synthesis route, specific studies were selected that were both highly cited and contained the most detailed information on FeO_x-NP characterization (i.e., size, shape, specific surface area, saturation magnetization). In the cases where substances for 1 Kg of FeO_x-NPs or Fe precursor synthesis were not found in the Ecoinvent database, those substances were broken down into their primary components as found in the Ecoinvent database. The total yield for FeO_x-NPs using biological methods was not reported in the literature. Therefore, a yield of 100% assuming ideal conditions was used.[26] The materials and input energy requirements to produce 1 kg of FeO_x-NPs and Fe precursors were calculated

based on a combination of the stoichiometry of the synthesis reactions and scale up of the data provided in the literature, as shown in **Figures S1-S8** and **Tables S1-S8.**

Table 1. Summarized information on functional units of the FeO_x-NPs produced by the seven mainstream lab-scale synthesis methods.

Synthesis route	Synthesis procedure	Precursor(s)	Mean particle diameter (nm)	Specific surface area ($m^2 g^{-1}$)	Saturation Magnetization M_s (emu g^{-1})	% yield used	Ref.
Chemical	Co-precipitation	$FeCl_3.6H_2O$, $FeCl_2$	10	63.5	75.3	100%	13, 34
	Thermal decomposition	FeO(OH)	7	150	38	95%	14, 35, 36
	Hydrothermal	$FeCl_2.4H_2O$	15.4	75.7[a]	53.3	90%	15, 37
	Sol-gel	$FeCl_3.6H_2O$	8.5	138	41	80%	16, 38, 39
	Electrochemical	$FeCl_3$	23	41.5	66	90%	18, 40
Physical	Flame spray pyrolysis (FSP)	$Fe(C_5H_7O_2)_3$ [$Fe(acac)_3$)]	16	94	38	80%	17, 41
Biological	Biological	$FeCl_3.6H_2O$	40	29.1[a]	75	100%	42, 43, 44, 45

$FeCl_3$ = Ferric chloride; **$FeCl_2$** = Ferrous chloride; **FeO(OH)** = Ferric OxyHydroxide; **$Fe(acac)_3$)** = Ferric acetylacetonate

[a] *Specific surface area was calculated using the reported mean particle size assuming spherically shaped particles and smooth surface morphology. Calculations were performed using eq (1).*

Functional Units

The primary functional unit considered in the LCA model for each of the synthesis routes and Fe precursors was 1 kg (mass-based) of FeO_x-NPs produced by each method, which allows for equivalent comparison across the nanomaterials described in the literature.[26, 27, 46] However, the use of only mass-based functional units is inadequate when considering changes in environmental impacts that arise due to the variable functional properties of FeO_x-NPs. Therefore, the relative impacts for each method were rescaled based on three additional functional units: mean particle diameter (nm), specific surface area (m^2/g), and saturation magnetization (M_s; emu/g)

(**Table 1**). Furthermore, the functional units in this study were utilized as 'declared units' since their use was limited to the normalization of the LCA dataset rather than to any NPs specific application. The mean particle diameter is a unique indicator of NP performance and can be controlled by varying the synthesis conditions. The mean particle diameters used in this study for all the synthesis methods have been reported in the literature based on transmission electron microscopy (TEM) measurements. M_s is defined as the maximum saturation magnetization of a material induced by a sufficiently large external magnetic field. M_s is one of the most important properties used to quantify the magnetic behavior of superparamagnetic materials and is often measured to be a function of particle size and temperature. The M_s (emu g^{-1}) values used for FeO_x-NPs for each synthesis method examined in this study were previously reported. In those cases where the BET (Brunauer–Emmett–Teller) specific surface area was not reported in the literature, eq (1) was used to calculate surface area, assuming NPs of roughly spherical shape and smooth surface.[26]

$$A = \frac{6}{(\rho \times d)} \quad (1)$$

where A = specific surface area (m^2/g), ρ = 5.15 g cm^{-3} for magnetite[13, 36] ; d = mean size (nm) for as-synthesized FeO_x-NPs.

Life Cycle Impact Assessment (LCIA)

For the LCA of environmental impacts, SimaPro (version 9.1.1) was used with the Ecoinvent (v3.6) database for inventory calculation. TRACI 2.1 (tool for the reduction and assessment of chemical and other environmental impacts, v1.05) was used for normalization (US 2008) and assessment of impacts. TRACI was chosen as a robust framework that can use the inventory of stressors (e.g., chemical requirements, energy use, etc.) to evaluate the land, air, and water environmental impacts, as well as resource depletion from FeO_x-NPs production using a set

of built-in impact categories (**Figure 1**).[47] The midpoint categories considered for impact assessment were ozone depletion (OD, kg CFC-11 equivalent), global warming potential (GW, kg CO_2 eq), smog (PS, kg O_3 eq), acidification (AC, mol SO_2 eq), eutrophication (EU, kg N eq), human health cancer (HHC, CTUh), human health non-cancer (HHNC, CTUh), respiratory effects (RE, kg $PM_{2.5}$ eq), ecotoxicity (EC, CTUe), and fossil fuel depletion (FF, MJ surplus). These midpoint categories are also consistent with the ones used in previous LCA studies on Ag and TiO_2 NPs synthesis methods, which enables comparison across different nanomaterials.[26, 27] For the energy required in all the syntheses for power, heating and mixing, we used the type of electricity in the Ecoinvent (v3.6) database designated as medium voltage electricity imported from the Northeast Power Coordinating Council (NPCC) in the US. Medium voltage electricity in SimaPro has been described as suitable for the production industry.[48] The release of FeO_x-NP waste to the Technosphere was not considered since it is not common practice to capture FeO_x-NP waste-streams in laboratory scale synthesis and disposal practices vary widely between labs. Nanomaterial waste streams, or nanowaste can be difficult to quantify since they are part of different wastes, such as industrial wastes, e-waste, plastic wastes, etc. However, the recovery and recycling of nanowaste has become popular concepts that need further development to become part of mainstream production techniques.[49, 50]

Interpretation

Energy Demand Calculations

Cumulative energy demand was calculated to compare the seven synthesis methods and six Fe precursors in terms of the direct and indirect energy utilization of the process. The cumulative energy demand (CED, v1.11) method, based on the ecoinvent 3.6 database in SimaPro, was used to calculate the energy demands in two non-renewable (fossil, nuclear) and four renewable (biomass, wind/solar/geothermal and water) categories. The total energy in MJ was the

sum of the energy demand in these six categories required to produce 1 kg of product (FeO_x-NPs or precursors). The components contributing to the energy demands were divided into three major categories: (1) processing, (2) chemicals/reagents, (3) Fe precursors.

Sensitivity and Uncertainty Analysis

Uncertainty analysis for each synthesis method was performed in SimaPro using the Monte Carlo method with 1000 runs and 95% confidence interval. The potential environmental impacts of each synthesis method were evaluated based on 60, 80, and 100% yields, assuming the materials and energy requirements would be higher for lower yields to produce the same 1 kg of FeO_x-NPs. Sensitivity analysis was conducted by varying the dominant contributors for each synthesis method by $\pm$25% and evaluating the corresponding percentage change in the midpoint impact categories.

Results and Discussion

Environmental Impacts of Producing Fe Precursors

Six Fe precursors were investigated with respect to their environmental and health effects. The relative environmental impacts of the precursors followed the general trend: $FeO(OH) > Fe(acac)_3 > Fe(CO)_5 > Fe(Cl)_3 \cdot 6H_2O > FeSO_4 > FeCl_2 \cdot 4H_2O$ (**Figure 2**). FeO(OH), $Fe(acac)_3$, and $Fe(CO)_5$ had higher environmental impacts compared to the other precursors across all categories and thus, were further analyzed to assess their process contributions (**Figure S9, Table S9**). Use of H_2O_2 (30% v/v) in the production of FeO(OH) was the main contributor to its overall environmental impacts in all categories except OD (**Figure S9**). H_2O_2 (30% v/v) is used to rapidly oxidize $Fe(OH)_2$ to produce feroxyhite (δ-Fe(O)OH).[51] Given that hydroperoxides are among the most widespread oxidants in earth's atmosphere, previous studies have linked the life cycle of H_2O_2 and its byproducts to adverse environmental impacts.[52, 53] For $Fe(CO)_5$ and $Fe(acac)_3$, respectively, carbon monoxide (CO) and sodium acetate (CH_3COONa) were the largest

contributors to the environmental and health impacts (**Figure S9**). Although it was not listed as one of the precursors for the synthesis processes studied here, $Fe(CO)_5$ has been used in other studies as a precursor for thermal decomposition synthesis of FeO_x-NPs and FeO_x-NP functionalized hybrid nanocomposites.[54, 55] The use of CO, a major component in the production of $Fe(CO)_5$, has adverse effects on the atmosphere as it is one of the most reactive trace gases that readily reacts with atmospheric hydroxyl (OH) radicals leading to their reduction.[56] $Fe(acac)_3$ is

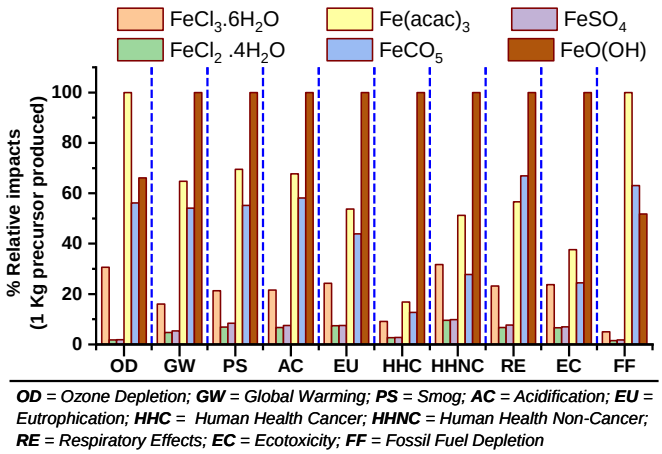

Figure 2. Comparison of relative environmental impacts of six Fe precursors across ten midpoint categories. Process contributions for FeO(OH), $Fe(acac)_3$ and $Fe(CO)_5$ are shown in **Table S9**.

often used as a Fe precursor for synthesis in nonpolar organic solvents. For $Fe(acac)_3$, sodium acetate (CH_3COONa) and methanol (CH_3OH) were the main contributors to its overall impacts (**Figure S9**). These two chemicals and the high energy used to produce 1 kg of $Fe(acac)_3$ resulted in a higher relative impact in the OD and FF midpoint category for $Fe(acac)_3$ compared to $Fe(CO)_5$ and FeO(OH) (**Figure 2**). In comparison, the inorganic precursors: $FeCl_3$•H_2O, $FeCl_2$•$4H_2O$ and $FeSO_4$ generated lower overall impacts across all categories. Previously, Wu et al. also found that the inorganic TiO_2 precursors had lower overall impacts compared to organic precursors.[26] The higher impacts of organic precursors primarily reflect the input chemicals and organic solvents required for their production. Since organic Fe precursors are increasingly being used for

engineered FeO_x-NP production, improvements in synthesis conditions and the use of less energy intensive chemicals can potentially lower the overall environmental and health impacts.

Impact Assessment of Seven Synthesis Methods

Seven FeO_x-NP synthesis methods were compared using four different functional units: mass, mean particle diameter, surface area, and saturation magnetization (**Figures 3 and S10, Tables S10-S13**). **Figures S1-S8** illustrate the synthesis processes for producing 1 kg of Fe precursors and FeO_x-NPs by each route. **Tables S1-S8** contain information on the inventories of all input materials and the energy requirements to produce 1 kg of Fe precursors and FeO_x-NPs by the seven methods.

Comparison by Different Functional Units

Results from the mass based relative environmental impacts followed the general trend: biological (100% yield)>thermal decomposition>FSP>sol-gel>electrochemical>hydrothermal >co-precipitation (**Figure 3a, Table S10**). Interestingly, the biological method had the highest environmental impact across all categories. The high energy requirements for bacterial culture media and energy for continuous operation of large-scale fermenters contribute to the high environmental impacts for the biological synthesis method. The FSP and thermal decomposition methods also generated high environmental impacts. The FSP method uses $Fe(acac)_3$ as an organic precursor mixed in xylene/acetonitrile solvent that is sprayed using a methane-oxygen flame. This combination of input chemicals along with the energy requirements for pyrolysis generated high impacts across all categories (**Figure 3a**). The thermal decomposition method generated the next highest impacts after the biological method across all categories except HHNC and FF. The use of nonpolar organic solvents with high boiling points to grow FeO_x-NPs at high temperature contributes to adverse environmental effects. The analysis of the sol-gel synthesis method suggests

that the combination of high solvent volumes for synthesis and the energy requirements for the gel drying process contributed to environmental impacts across all categories (**Figure 3a**, **Table S5**). For hydrothermal, electrochemical, and co-precipitation methods, the overall chemicals and energy requirements were lower, thus resulting in lower environmental and health impacts across all categories.

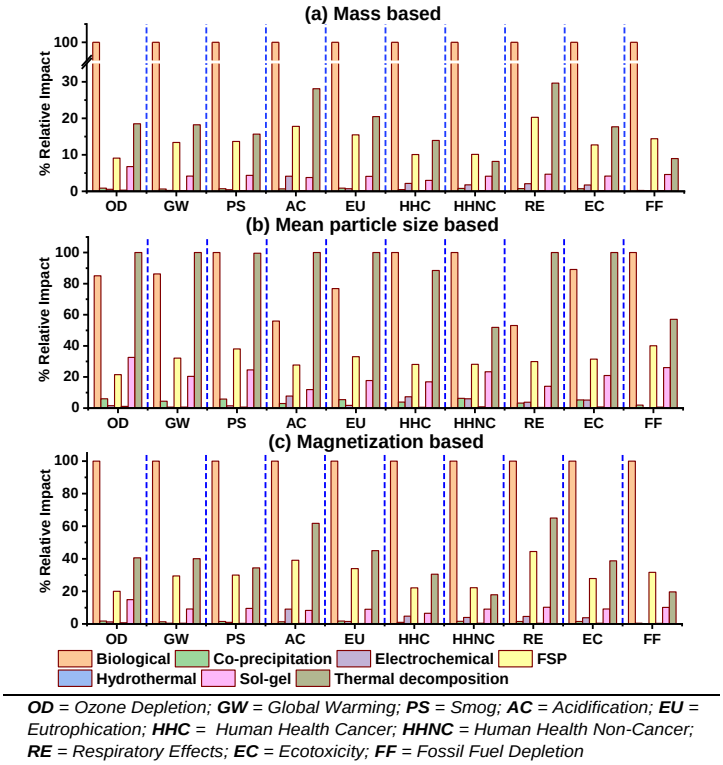

Figure 3. The relative environmental impacts across ten midpoint categories normalized based on **(a)** mass, **(b)** mean particle diameter and **(c)** saturation magnetization. For (**a**), a scale bar cutoff has been introduced on the y-axis due to the large difference between the least and the most impact generated synthesis methods. Surface area based relative impacts showed similar trends to the mass-based impacts are shown in **Figure S10**.

When considering the functionality of FeO_x-NPs produced via different synthesis methods, mass-based comparisons alone are inadequate. NP applications such as adsorption and surface functionalization are often driven by particle size and specific surface area, which are relevant indicators of their performance. Interestingly, when the relative environmental impacts were rescaled based on mean particle size, thermal decomposition was the worst performing synthesis

method with the highest relative impacts across six categories: OD, GW, AC, EU, RE and EC (**Figure 3b, Table S11**). The biological method came in second with highest impacts in PS, HHC, HHNC and FF categories, due to the high impact offset by the corresponding FeO_x-NP mean particle size of 40 nm, largest among FeO_x-NPs produced by the seven methods. The thermal decomposition method incorporates synthesis in non-polar solvents and the use of stabilizing or capping agents such as oleic acid that provide more precise control over the shape and diameter of FeO_x-NPs, which can be as small as 6-7 nm.[57] The reduction in particle size can lead to higher surface areas, thereby improving FeO_x-NP sorption capacity. For comparison, the biological method produces magnetosomes that are biomineralized FeO_x-NPs surrounded by lipid vesicles, hence contributing to their larger overall diameters of 30-120 nm.[44] The relative impacts of the FSP and sol-gel methods increased by 9.9 to 25.7% and 8.1 to 25.8% across all impact categories (**Figure 3b**). The co-precipitation, hydrothermal, and electrochemical methods showed a low increase (<6%) in all impact categories. The relative environmental impacts, when rescaled based on specific surface area, followed a similar trend to that of the mass based functional units (**Figure S10, Table S12**). The biological method generated the highest relative impacts, followed by the other synthesis methods. While the relative impacts are normalized based on the functional units presented in **Table 1**, it is possible to produce FeO_x-NPs of different sizes and surface areas using a single synthesis method by varying the synthesis conditions. Based on a specific functional unit and application, the relative impacts can be rescaled accordingly.

When the data were rescaled based on the saturation magnetization (emu g^{-1}) of the FeO_x-NPs, the synthesis methods followed the same general trend in terms of their relative impacts relative to the impacts based on mass based functional units (**Figure 3c, Table S13**). The only exception was that the hydrothermal method replaced the co-precipitation method as the least

environmentally intensive. However, several synthesis methods showed an increase in their relative impacts due to the variation in the saturation magnetization of FeO_x-NPs produced by the different methods. The thermal decomposition and FSP methods showed 9.7 to 33.6% and 10.9 to 21.3% increase across all midpoint categories. The sol-gel method showed 3.6 to 8.1% increase across all categories. The co-precipitation, hydrothermal, and electrochemical methods were again consistent in showing low increases (< 3%) in all impact categories. Results from the comparison of FeO_x-NP synthesis methods suggest that consideration of activity based functional units is highly important when evaluating the relative environmental impacts of each method. Adequate selection of functional units is strongly recommended when analyzing NP production processes and applications using LCA.

Breakdown of Process Contribution

To better understand which components of the synthesis processes most greatly influenced their overall environmental and health impacts, each synthesis method was analyzed in terms of process contributors and the results are presented in **Figure 4**. For the biological method, lactic acid constituted 74.7 to 86.2% of the process impact across all categories. Lactic acid, a primary component in bacterial culture media, serves as a carbon source and electron donor in the bacterial growth process. The fermentation and storage of lactic acid have been previously identified to be energy and environmentally intensive.[58] The input chemicals and the energy required for the biological method were calculated based on the 356.6 mg L^{-1} yield suggested by Zhang et al. and 100% of the Fe (III) precursor ($FeCl_3 \cdot 6H_2O$) was assumed to be converted to NPs.[43]

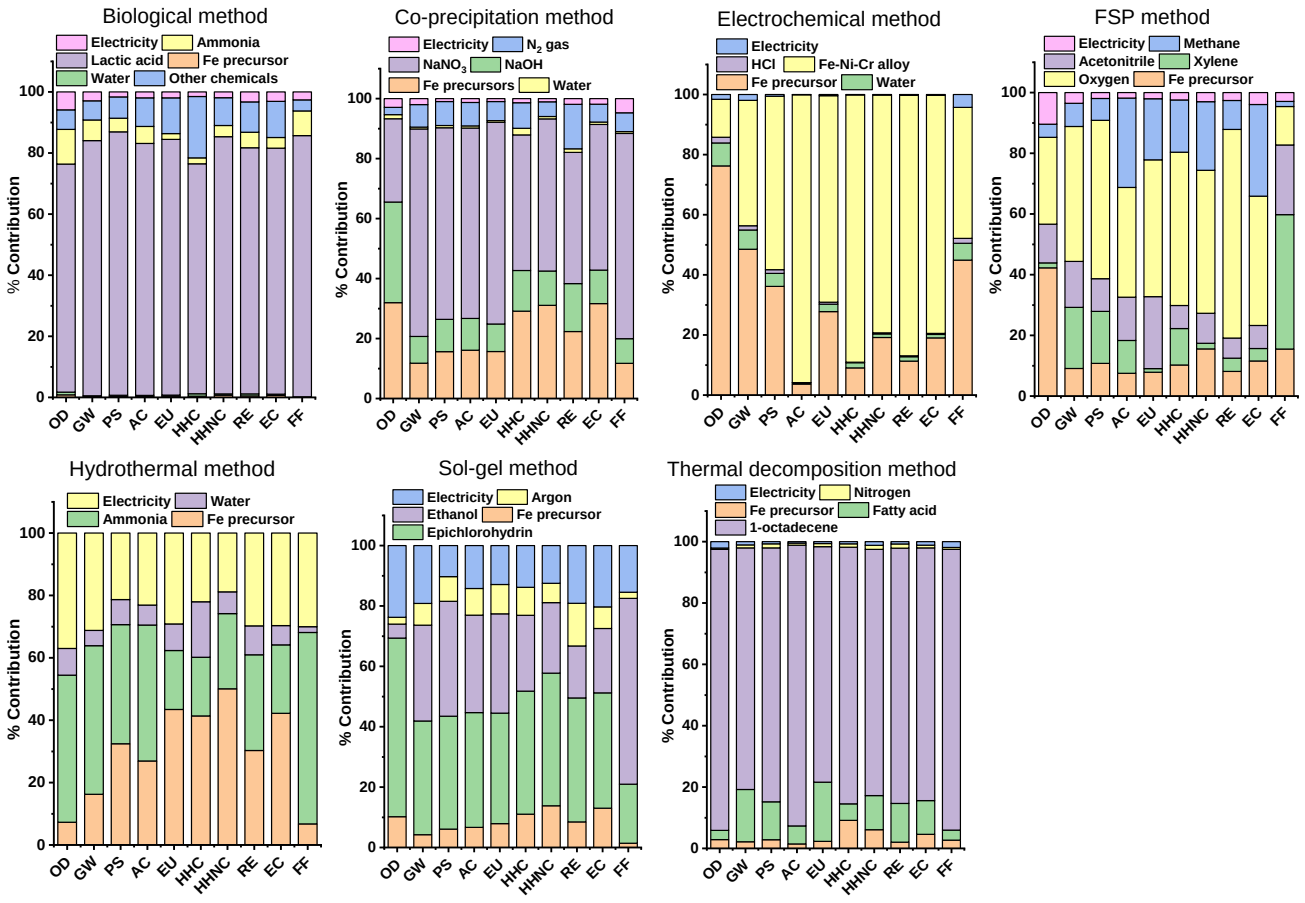

***OD** = Ozone Depletion; **GW** = Global Warming; **PS** = Smog; **AC** = Acidification; **EU** = Eutrophication; **HHC** = Human Health Cancer; **HHNC** = Human Health Non-Cancer; **RE** = Respiratory Effects; **EC** = Ecotoxicity; **FF** = Fossil Fuel Depletion*

Figure 4. Breakdown of process contributions to the overall environmental impacts across ten midpoint categories for seven FeO_x-NP synthesis methods.

Even with a 100% production yield as assumed for this study, there is ≈2800 kg of water required in the continuous feed solution for cell growth and magnetosome formation to produce 1 kg of FeO_x-NPs (**Table S8**). Furthermore, the optimal combination of bacterial feed for shake-flask culture is not directly applicable to laboratory scale fermentation and research is developing on the effects of growth media and environmental conditions on maximizing bacteria yield.[22, 59, 60] Therefore, the yield of magnetosomes using laboratory fermentation techniques needs additional improvements before biological synthesis of FeO_x-NPs can achieve the desired level of efficiency to compete with other mainstream synthesis methods.

The use of a large amount of non-polar organic solvent (1-octadecene) to synthesize 1 kg of FeO_x-NPs in the thermal decomposition method accounted for 76.8 to 91.6% of the process contribution across all categories (**Figure 4**). Non-polar organic solvents are generally immiscible in water and the hazards associated with these chemicals are generally airborne emissions.[61, 62] Previous studies investigated chemical risk assessment of solvents using several approaches such as environmental health and safety (EHS), LCA, and multi-criteria decision analysis (MCDA) to provide a 'greenness' ranking indicator for solvents.[61, 63] Results from these studies have shown that chlorinated and aromatic hydrocarbons pose a greater environmental risk than alcohols and esters.[61, 63] The use of recyclable and reusable imidazole-based ionic solvents can be potentially explored as greener alternatives for energy intensive non-polar organic.[64, 65] However, LCA on ionic liquids and their applications suggest further improvement is needed in their separation efficiency, recyclability, and stability.[66] While the thermal decomposition method yields reproducible and highly crystalline FeO_x-NPs with control over size and shape, finding more sustainable pathways for the production of precursor organic solvents will contribute to lowering their environmental and health effects.

As a physical route of synthesis, the FSP method had supporting gases (oxygen/methane for atomization) contributing from 52.1 to 78.3% across all categories except OD (32.9%) and FF (14.4%) (**Figure 4**). Precursor solvents (xylene/acetonitrile) contributed from 11 to 35.3% across all categories except in FF, where it was the main contributor with a 67.3% contribution. Unsurprisingly, $Fe(acac)_3$, which had the highest impacts in the OD and FF category among all Fe precursors (**Figure 2**), was the highest contributor in the OD category with 42.3%. The combustion of the supporting gases and high electricity requirements for pyrolysis are the main contributors to

environmental impacts of the FSP method. Streamlining the production process for efficient use of input chemicals and capturing of gas emissions can potentially reduce these impacts.

The relative impacts from the other methods apart from the biological, thermal decomposition and FSP were comparatively lower (**Figure 3a-3c**). The high energy requirements for the drying process and high solvent (epichlorohydrin/ethanol) requirements of the sol-gel method contributed 77.4 to 88.6% across all impact categories (**Figure 4**). For the hydrothermal method, high energy for autoclave operation and input chemical (ammonia and Fe precursor) requirements contributed 82.2 to 98.1% across all impact categories. The energy requirements for the co-precipitation and electrochemical methods were low compared to the Fe precursor and input chemicals, which contributed 82.1 to 93.3% and 88.9 to 99.4%, respectively, for these two methods across all impact categories (**Figure 4**). To summarize, the thermal decomposition (chemical route), FSP (physical route), and biological methods had the highest environmental impacts for FeO_x-NP synthesis. Further research is needed to improve synthesis yield and optimize energy and input chemical requirements to ensure development of environmentally sustainable FeO_x-NP production process.

Cumulative Energy Demand

Cumulative Energy Demand (CED) represents the direct and indirect energy (MJ) use of a material throughout its life cycle. CED is calculated as the total of non-renewable (fossil fuel and nuclear) and renewable (biomass, wind/solar/geothermal and water) CEDs in the life cycle. CED has been suggested as an acceptable single score predictor of environmental impacts of a variety of materials such as metals, glass, paper, chemicals, and plastics.[67, 68] Among the six Fe precursors compared, the three environmentally intensive precursors: $Fe(acac)_3$, $Fe(CO)_5$, and FeO(OH) had CEDs of 120.4, 92.5, and 89.1 MJ/kg for production (**Figure 5b, Table S14**). In comparison, the inorganic Fe precursors: $FeCl_3.6H_2O$, $FeCl_2$ and $FeSO_4$ had very low energy requirements (<13

MJ/kg). Previously, Sadhukhan et al. performed LCA and reported lower environmental impacts when $FeCl_3$ is replaced by $FeSO_4$ as the Fe precursor in magnetite bionanoparticle production.[69] The CED of the seven synthesis methods followed the trend: biological (100% yield)>thermal decomposition>FSP>sol-gel>co-precipitation>hydrothermal>electrochemical (**Figure 5a, Table S15**). For all precursors and synthesis methods, the use of chemicals were the major contributors to the CED (**Figure 5**a,**5b**). For the biological, FSP, and sol-gel methods, there were substantial contributions to the CED from processing energy requirements. The use of a particular type of electricity in the Ecoinvent database did not have a major effect on the overall CED score. The precursor $Fe(CO)_5$ production requires energy to maintain high temperature and pressure conditions, which contributed to the CED (**Figure 5b**).

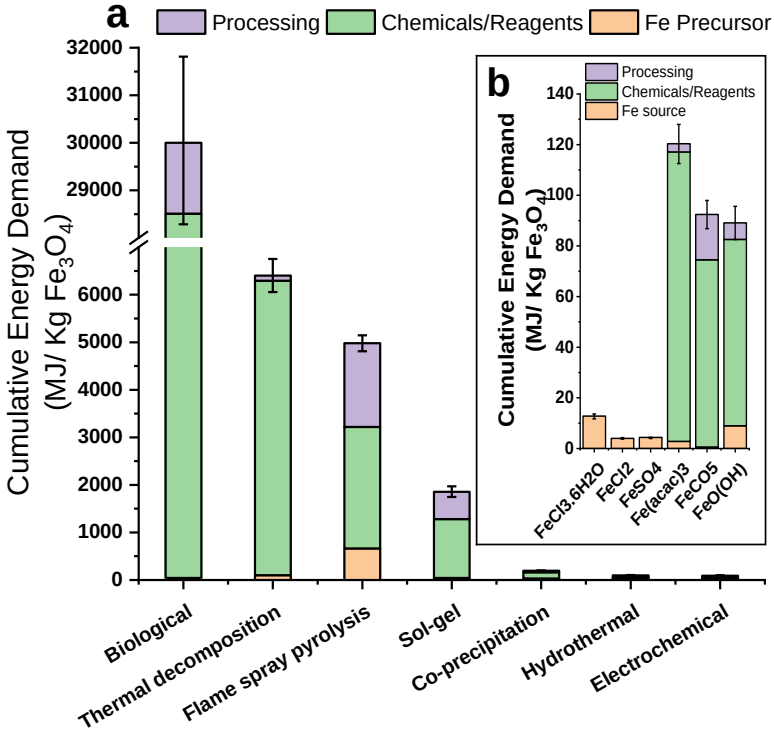

Figure 5. Cumulative energy demand of **(a)** seven synthesis methods to produce 1 kg of FeO_x-NPs and **(b)** six Fe precursors used in FeOx-NP synthesis. In figure **(a)**, A scale bar cutoff has been introduced on the y-axis due to the large difference between the CED of the biological (100% yield assumed) and other synthesis methods. Uncertainties are indicated by error bars.

Sensitivity and Uncertainty Analysis

The mean environmental impacts (mass, mean particle diameter, and magnetization based) across ten impact categories for the seven synthesis methods along with the associated uncertainties, as indicated by the upper and lower bound values, are presented in **Figure S11**. Based on the mass based functional unit, the biological, thermal decomposition and FSP routes showed higher mean environmental impacts across all impact categories than the other methods. For all the synthesis methods, lower yields of 80 and 60% caused environmental impacts across the ten categories to rise by ≈25% and ≈67% respectively (**Table S16**). This data shows the importance of achieving high yields in the production process to greatly reduce environmental impacts. The dominant components: lactic acid (**Figure 6a**), 1-octadecene (**Figure 6b**), and methane-oxygen input gas (**Figure 6c**) were varied by ±25% to evaluate the sensitivity of the corresponding three most environmentally intensive synthesis methods (i.e., biological, thermal decomposition, and FSP) to these changes. The results showed substantial increase/decrease in percent change across ten impact categories (~ 18 to 22% for the biological, ~ 18 to 27% for the thermal decomposition, and ~ 3 to 20% for the FSP synthesis method) to the corresponding increase/decrease in dominant components (**Figure 6, Table S17**). The results for the four other synthesis methods are presented in **Figure S12**. Thus, identifying potential hotspots in the life cycle of FeO_x-NP production processes can greatly reduce overall environmental impacts.

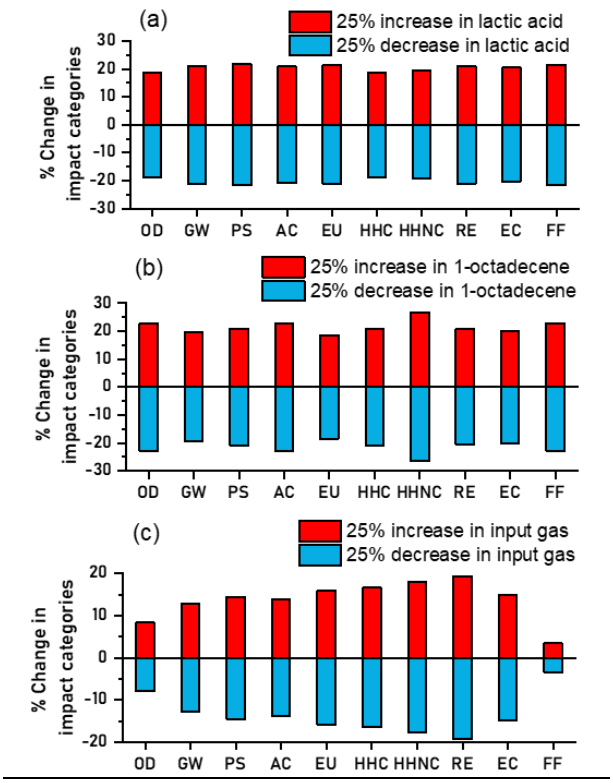

Figure 6. The sensitivity of the biological, FSP and thermal decomposition synthesis methods to ± 25% change in their corresponding dominating contributors: lactic acid, 1-octadecene and input gas (Methane+Oxygen). Sensitivity was measured through percent change in ten midpoint categories.

Conclusions

The data presented in this study offer a holistic approach of looking across FeO_x-NP synthesis methods and comparing them using LCA. The in-depth analysis of the FeO_x-NP synthesis methods and the LCA inventory data provided here will help address the very limited existing knowledge on LCA approaches for FeO_x-NP synthesis and environmental impacts. In general, the synthesis methods involving chemical routes (i.e., co-precipitation, hydrothermal, electrochemical, and sol-gel) were less environmentally intensive due to lower requirements for energy and chemicals for processing. Previously, the LCA of synthesis routes of AgNPs and TiO_2 NPs also indicated the comparatively higher environmental impacts of physical and biological

synthesis routes.[26, 27] In this study, however, the thermal decomposition method was an exception to this general trend due to the high energy requirements of non-polar organic solvents required for synthesis, resulting in high environmental impacts. FSP, a physical method, requires considerably higher electricity and input gas for processing, hence resulting in high environmental impacts. The high amount of lactic acid as well as water and electricity requirements primarily contributed to the highest environmental impacts among the synthesis methods resulting from biological synthesis of FeO_x-NPs. Further research is required to improve the energy input and yields for biological synthesis methods to achieve more instructive comparisons with the other synthesis methods.

In reality, however, environmental impact is not the only criterion for the selection of a particular FeO_x-NP synthesis method. There are many other factors, such as product quality (e.g., particle diameter, shape, surface area, magnetization), ease of use, cost, processing time, equipment availability, and intended application that are considered when selecting a synthesis process. For example, despite their high energy requirements, FeO_x-NPs produced by thermal decomposition are often desired for pollutant removal and environmental sensing applications due to their high reactivity, size tunability, and magnetic response.[8, 9, 35] Biological synthesis of FeO_x-NPs is often used to study the biomineralization of magnetic minerals, which can provide insights into certain physiological processes, such as the strengthening of tissues.[70, 71] **Table 2** lists the advantages and disadvantages of each synthesis method, along with the CED values reported in this study. This summarized information provides a clearer understanding of the potential tradeoffs between applicability and environmental impacts associated with FeO_x-NP synthesis. The increasing use of FeO_x-NPs as important nanomaterials for technology, research, and industrial

applications emphasize the need for a comprehensive understanding of the potential environmental and health impacts of these nanomaterials.

While the LCA presented in this study based on lab-scale FeO_x-NP synthesis methods provides a comprehensive understanding of potential contributors to harmful environmental impacts, it is important to consider the limitations of extrapolating lab-scale synthesis to industrial conditions. For example, the characteristics of the FeO_x-NPs might be different when produced industrially. The potential release and exposure to NP waste could also be more significant under industrial conditions. A goal of future work should be to better understand the environmental impacts of FeO_x-NP synthesis methods under more realistic production conditions, where large scale synthesis may offer economies of scale that lower overall impacts and energy requirements.[72, 73] The recovery and recycling of nanowaste should be standardized which can significantly reduce the environmental impacts of NPs synthesis. Nevertheless, this LCA study underscores areas in the FeO_x-NP synthesis methods with potential for future improvement in efficiency, such as the selection of less environmentally intensive Fe precursors, prudent use of key synthesis ingredients/solvents, and streamlining of the overall process for lower energy requirements. The inventory and analysis of lab scale synthesis presented here can be useful for potential future works on developing sustainable industrial scale production of FeO_x-NPs.

Table 2. Summary of the FeO_x-NP synthesis routes: advantages, disadvantages and the CEDs

Synthesis route	Advantages	Disadvantages	CED (MJ/kg)	Ref.
Co-precipitation	Most widely used method for simple synthesis and washing processes; Low energy and chemical requirements; Easy to scale up for large quantity synthesis.	Intermediate phases found in the final product; Hard to control size and shape of the particles; NPs tend to aggregate easily in aqueous suspensions.	1.97×10^2	13, 34
Thermal decomposition	Precise control over the size and shape of FeO_x-NPs; NPs are homogeneously dispersed in organic solvents; Organic layer capped FeO_x-NPs are protected from oxidation.	High requirements for energy, temperature, and non-polar organic solvents; Complex synthesis setup; Thickness of the capping agent can affect NP magnetic properties.	6.40×10^3	9, 14, 35, 57
Hydrothermal	Produces highly crystalline and homogenous NPs; A great alternative to the thermal decomposition process for size and shaped controlled FeO_x-NP synthesis; Synthesized NPs can be readily suspended in aqueous suspensions.	Requires expensive autoclaves; Lengthy duration of synthesis in high temperature and pressure and the subsequent cooling; Pressurized closed reactor inhibits control of reaction process.	9.64×10^1	15, 37
Sol-gel	Good control over the size and shape of NPs; Homogeneity for both the 'sol' and the 'gel' system due to the mixing in liquid medium; Low temperature required for solution processing.	NPs can contain impurities (i.e., aggregates, intermediate products); Lengthy processing time; Shrinkage after gel drying results in lower yield; High temperature required for gel drying.	1.85×10^3	16, 38, 39
Electro-chemical	Size, shape and production rate of the NPs can be controlled by varying the electrochemical conditions; High magnetic saturation in particles; Low temperature synthesis.	Cathode material (Fe alloy) has adverse environmental impacts; Poorly crystalline products which can be hard to characterize; NPs often contain amorphous impurities.	9.20×10^1	18, 40
FSP	Rapid, one-step technique; Produces low amount of waste; Highly scalable; High production rate with control over particle size.	Requires high energy and input gas; Expensive synthesis apparatus; Often produces aggregated particles that exhibit low saturation magnetization.	4.98×10^3	17, 41
Biological	Study of biomineralization; Large scale cultivation possible through continuous feed-batch process; Low use of toxic chemicals; Magnetosomes have high saturation magnetization and have great potential as nanocarriers in biotechnology.	Large-scale cultivation is still developing; Isolation and characterization of magnetosomes are challenging; High amount of bacterial culture media, and high energy and water requirements; Low and inconsistent yield.	3.00×10^4	22, 42, 43, 59, 69

Acknowledgements

This work was supported by the Virginia Tech Graduate School Sustainable Nanotechnology Interdisciplinary Graduate Engineering Program (VTSuN-IGEP).

Supporting Information Available

Detailed description of the synthesis methods, stoichiometry, calculations, and assumptions, 17 additional tables (S1 to S17) and 12 additional figures (S1 to S12) are provided. This material is available free of charge at http://pubs.acs.org.

References

(1) Wu, W.; He, Q.; Jiang, C. Magnetic iron oxide nanoparticles: synthesis and surface functionalization strategies**.** *Nanoscale Res. Lett.* **2008**, *3* (11), 397–415.

(2) Pankhurst, Q. A.; Connolly, J.; Jones, S. K.; Dobson, J. Applications of magnetic nanoparticles in biomedicine. *J. Phys. D: Appl. Phys*. **2003**, *36* (13), R167.

(3) Laurent, S.; Forge, D.; Port, M.; Roch, A.; Robic, C.; Vander Elst, L.; Muller, R. N., Magnetic iron oxide nanoparticles: synthesis, stabilization, vectorization, physicochemical characterizations, and biological applications. *Chem. Rev.* **2008**, *108* (6), 2064-2110.

(4) Abdelsalam, E.; Samer, M.; Attia, Y.; Abdel-Hadi, M.; Hassan, H.; Badr, Y. Influence of zero valent iron nanoparticles and magnetic iron oxide nanoparticles on biogas and methane production from anaerobic digestion of manure. *Energy* **2017**, *120*, 842-853.

(5) Jain, T. K.; Morales, M. A.; Sahoo, S. K.; Leslie-Pelecky, D. L. Labhasetwar, V. Iron oxide nanoparticles for sustained delivery of anticancer agents. *Mol. Pharm.* **2005**, *2* (3), 194-205.

(6) Peterson, R. D.; Cunningham, B. T.; Andrade, J. E. A photonic crystal biosensor assay for ferritin utilizing iron-oxide nanoparticles. *Biosens. Bioelectron.* **2014**, *56*, 320-327.

(7) Hasanzadeh, M.; Shadjou, N.; de la Guardia, M. Iron and iron-oxide magnetic nanoparticles as signal-amplification elements in electrochemical biosensing. *TrAC, Trends Anal. Chem.* **2015**, *72*, 1-9.

(8) Kim, C.; Lee, S. S.; Lafferty, B. J.; Giammar, D. E.; Fortner, J. D. Engineered superparamagnetic nanomaterials for arsenic (V) and chromium (VI) sorption and separation: quantifying the role of organic surface coatings. *Environ. Sci. Nano* **2018**, *5* (2), 556-563.

(9) Li, W.; Troyer, L. D.; Lee, S. S.; Wu, J.; Kim, C.; Lafferty, B. J.; Catalano, J. G.; Fortner, J. D. Engineering nanoscale iron oxides for uranyl sorption and separation: Optimization of particle core size and bilayer surface coatings. *ACS Appl. Mater. Interfaces* **2017**, *9* (15), 13163-13172.

(10) *Grand View Research, Magnetite Nanoparticles Market Report Scope,* https://www.grandviewresearch.com/industry-analysis/magnetite-nanoparticles-market *(accessed 2021-05-19)*

(11) Teja, A. S.; Koh, P.-Y. Synthesis, properties, and applications of magnetic iron oxide nanoparticles. *Prog. Cryst. Growth Charact. Mater.* **2009**, *55* (1-2), 22-45.

(12) Qiao, R.; Yang, C.; Gao, M. Superparamagnetic iron oxide nanoparticles: from preparations to in vivo MRI applications. *J. Mater. Chem.* **2009**, *19* (35), 6274-6293.

(13) Vikesland, P. J.; Heathcock, A. M.; Rebodos, R. L.; Makus, K. E. Particle size and aggregation effects on magnetite reactivity toward carbon tetrachloride. *Environ. Sci. Technol.* **2007**, *41* (15), 5277-5283.

(14) William, W. Y.; Falkner, J. C.; Yavuz, C. T.; Colvin, V. L. Synthesis of monodisperse iron oxide nanocrystals by thermal decomposition of iron carboxylate salts. *Chem. Commun.* **2004**, (20), 2306-2307.

(15) Ge, S.; Shi, X.; Sun, K.; Li, C.; Uher, C.; Baker Jr, J. R.; Banaszak Holl, M. M.; Orr, B. G. Facile hydrothermal synthesis of iron oxide nanoparticles with tunable magnetic properties. *J. Phys. Chem. C* **2009**, *113* (31), 13593-13599.

(16) Long, J. W.; Logan, M. S.; Rhodes, C. P.; Carpenter, E. E.; Stroud, R. M.; Rolison, D. R. Nanocrystalline iron oxide aerogels as mesoporous magnetic architectures. J. Am. Chem. Soc. **2004**, *126*, (51), 16879-16889.

(17) Li, D.; Teoh, W. Y.; Selomulya, C.; Woodward, R. C.; Munroe, P.; Amal, R. Insight into microstructural and magnetic properties of flame-made γ-Fe 2 O 3 nanoparticles. *J. Mater. Chem.* **2007**, *17* (46), 4876-4884.

(18) Park, H.; Ayala, P.; Deshusses, M. A.; Mulchandani, A.; Choi, H.; Myung, N. V. Electrodeposition of maghemite (γ-Fe2O3) nanoparticles. *Chem. Eng. J.* **2008**, *139* (1), 208-212.

(19) Gao, S.; Shi, Y.; Zhang, S.; Jiang, K.; Yang, S.; Li, Z.; Takayama-Muromachi, E. Biopolymer-assisted green synthesis of iron oxide nanoparticles and their magnetic properties. *J. Phys. Chem. C* **2008**, *112* (28), 10398-10401.

(20) Martínez-Cabanas, M.; López-García, M.; Barriada, J. L.; Herrero, R.; de Vicente, M. E. S. Green synthesis of iron oxide nanoparticles. Development of magnetic hybrid materials for efficient As (V) removal. *Chem. Eng. J.* **2016**, *301*, 83-91.

(21) Shahwan, T.; Sirriah, S. A.; Nairat, M.; Boyacı, E.; Eroğlu, A. E.; Scott, T. B.; Hallam, K. R. Green synthesis of iron nanoparticles and their application as a Fenton-like catalyst for the degradation of aqueous cationic and anionic dyes. *Chem. Eng. J.* **2011**, *172* (1), 258-266.

(22) Liu, Y.; Li, G. R.; Guo, F. F.; Jiang, W.; Li, Y.; Li, L. J. Large-scale production of magnetosomes by chemostat culture of Magnetospirillum gryphiswaldense at high cell density. *Microb. cell fact.* **2010**, *9* (1), 99.

(23) Ayres, R. U. Life cycle analysis: A critique. *Resour. Conserv. Recycl.* **1995**, *14* (3-4), 199-223.

(24) Theis, T. L.; Bakshi, B. R.; Durham, D.; Fthenakis, V. M.; Gutowski, T. G.; Isaacs, J. A.; Seager, T.; Wiesner, M. R. A life cycle framework for the investigation of environmentally benign nanoparticles and products. *Phys. Status Solidi - Rapid Res. Lett.* **2011**, *5* (9), 312-317.

(25) Grubb, G. F.; Bakshi, B. R. Life cycle of titanium dioxide nanoparticle production: Impact of emissions and use of resources. *J. Ind. Ecol.* **2011**, *15* (1), 81-95.

(26) Wu, F.; Zhou, Z.; Hicks, A. L. Life cycle impact of titanium dioxide nanoparticle synthesis through physical, chemical, and biological routes. *Environ. Sci. Technol.* **2019**, *53* (8), 4078-4087.

(27) Pourzahedi, L.; Eckelman, M. J. Comparative life cycle assessment of silver nanoparticle synthesis routes. *Environ. Sci. Nano* **2015**, *2* (4), 361-369.

(28) Leng, W.; Pati, P.; Vikesland, P. J. Room temperature seed mediated growth of gold nanoparticles: mechanistic investigations and life cycle assesment. *Environ. Sci. Nano* **2015**, *2* (5), 440-453.

(29) 17.Feijoo, S.; González-García, S.; Moldes-Diz, Y.; Vazquez-Vazquez, C.; Feijoo, G.; Moreira, M. Comparative life cycle assessment of different synthesis routes of magnetic nanoparticles. *J. Clean. Prod.* **2017**, *143*, 528-538.

(30) Marimón-Bolívar, W.; González, E. E. Green synthesis with enhanced magnetization and life cycle assessment of Fe3O4 nanoparticles. *Environ. Nanotechnol. Monit. Manag.* **2018**, *9*, 58-66.

(31) Singh, N.; Jenkins, G. J.; Asadi, R.; Doak, S. H. Potential toxicity of superparamagnetic iron oxide nanoparticles (SPION). *Nano Rev.* **2010**, *1* (1), 5358.

(32) Soenen, S. J.; De Cuyper, M. Assessing iron oxide nanoparticle toxicity in vitro: current status and future prospects. *Nanomedicine* **2010**, *5*, (8), 1261-1275.

(33) Liu, G.; Gao, J.; Ai, H.; Chen, X. Applications and potential toxicity of magnetic iron oxide nanoparticles. *Small* **2013**, *9*, (9-10), 1533-1545.

(34) Rebodos, R. L.; Vikesland, P. J. Effects of oxidation on the magnetization of nanoparticulate magnetite. *Langmuir* **2010**, *26*, (22), 16745-16753.

(35) Li, W.; Lee, S. S.; Wu, J.; Hinton, C. H.; Fortner, J. D. Shape and size controlled synthesis of uniform iron oxide nanocrystals through new non-hydrolytic routes. *Nanotechnology* **2016**, *27*, (32), 324002.

(36) Pan, Z.; Li, W.; Fortner, J. D.; Giammar, D. E. Measurement and surface complexation modeling of U (VI) adsorption to engineered iron oxide nanoparticles. *Environ. Sci. Technol* **2017**, *51*, (16), 9219-9226.

(37) Daou, T.; Pourroy, G.; Bégin-Colin, S.; Greneche, J.-M.; Ulhaq-Bouillet, C.; Legaré, P.; Bernhardt, P.; Leuvrey, C.; Rogez, G. Hydrothermal synthesis of monodisperse magnetite nanoparticles. *Chem. Mater.* **2006**, *18*, (18), 4399-4404.

(38) Duraes, L.; Costa, B.; Vasques, J.; Campos, J.; Portugal, A. Phase investigation of as-prepared iron oxide/hydroxide produced by sol–gel synthesis. *Mater. Lett.* **2005**, *59* (7), 859-863.

(39) Silva, M. F.; de Oliveira, L. A.; Ciciliati, M. A.; Silva, L. T.; Pereira, B. S.; Hechenleitner, A. A. W.; Oliveira, D. M.; Pirota, K. R.; Ivashita, F. F.; Paesano Jr, A. Nanometric particle size and phase controlled synthesis and characterization of γ-Fe2O3 or (α+ γ)-Fe2O3 by a modified sol-gel methodInt. *J. Appl. Phys.* **2013**, *114* (10), 104311.

(40) Starowicz, M.; Starowicz, P.; Żukrowski, J.; Przewoźnik, J.; Lemański, A.; Kapusta, C.; Banaś, J. Electrochemical synthesis of magnetic iron oxide nanoparticles with controlled size. *J. Nanoparticle Res.* **2011**, *13* (12), 7167-7176.

(41) Li, D.; Teoh, W. Y.; Selomulya, C.; Woodward, R. C.; Amal, R.; Rosche, B. Flame-sprayed superparamagnetic bare and silica-coated maghemite nanoparticles: Synthesis, characterization, and protein adsorption− desorption. *Chem. Mater.* **2006**, *18* (26), 6403-6413.

(42) Faivre, D.; Schuler, D. Magnetotactic bacteria and magnetosomes. *Chem. Rev.* **2008**, *108* (11), 4875-4898.

(43) Zhang, Y.; Zhang, X.; Jiang, W.; Li, Y.; Li, J. Semicontinuous culture of Magnetospirillum gryphiswaldense MSR-1 cells in an autofermentor by nutrient-balanced and isosmotic feeding strategies. *Appl. Environ. Microbiol.* **2011**, *77* (17), 5851-5856.

(44) Liu, R.-t.; Liu, J.; Tong, J.-q.; Tang, T.; Kong, W.-C.; Wang, X.-w.; Li, Y.; Tang, J.-t. Heating effect and biocompatibility of bacterial magnetosomes as potential materials used in magnetic fluid hyperthermia. *Prog. Nat. Sci.: Mater.* **2012**, *22*, (1), 31-39.

(45) Staniland, S.; Williams, W.; Telling, N.; Van Der Laan, G.; Harrison, A.; Ward, B. Controlled cobalt doping of magnetosomes in vivo. *Nat. Nanotechnol* **2008**, *3* (3), 158.

(46) Hischier, R.; Walser, T., Life cycle assessment of engineered nanomaterials: state of the art and strategies to overcome existing gaps. *Sci. Total Environ.* **2012**, *425*, 271-282.

(47) Bare, J.; Young, D.; QAM, S.; Hopton, M.; Chief, S. A. B., *Tool for the Reduction and Assessment of Chemical and other Environmental Impacts (TRACI)*; EPA/600/R-12/554; United States Environmental Protection Agency, Sustainable Technology Division: Cincinnati, OH 45268. https://nepis.epa.gov/Adobe/PDF/P100HN53.pdf (accessed 2022-02-03).

(48) Understanding electricity in SimaPro. [Online]. Available: https://simapro.com /2019/understanding-electricity-in-simapro/ (accessed 2022-02-03).

(49) Abdelbasir, S. M.; McCourt, K. M.; Lee, C. M.; Vanegas, D. C., Waste-derived nanoparticles: synthesis approaches, environmental applications, and sustainability considerations. *Front. Chem.* **2020**, *8*, 782.

(50) Pati, P.; McGinnis, S.; Vikesland, P. J., Waste not want not: life cycle implications of gold recovery and recycling from nanowaste. *Environ. Sci. Nano* **2016**, *3*, (5), 1133-1143.

(51) Schwertmann, U.; Cornell, R. M. *Iron oxides in the laboratory: preparation and characterization*; John Wiley & Sons, 2008.

(52) Castiello, D.; Puccini, M.; Seggiani, M.; Vitolo, S.; Zammori, F. Life Cycle Assessment (LCA) of the oxidative unhairing process. *J. Am. Leather Chem. Assoc.* **2008**, *103* (01), 1-6.

(53) Jackson, A.; Hewitt, C. Atmosphere hydrogen peroxide and organic hydroperoxides: a review. *Crit. Rev. Environ. Sci. Technol* **1999**, *29* (2), 175-228.

(54) Moisala, A.; Nasibulin, A. G.; Brown, D. P.; Jiang, H.; Khriachtchev, L.; Kauppinen, E. I. Single-walled carbon nanotube synthesis using ferrocene and iron pentacarbonyl in a laminar flow reactor. *Chem. Eng. Sci.* **2006**, *61*, (13), 4393-4402.

(55) Jiang, G.; Huang, Y.; Zhang, S.; Zhu, H.; Wu, Z.; Sun, S. Controlled synthesis of Au–Fe heterodimer nanoparticles and their conversion into Au–Fe 3 O 4 heterostructured nanoparticles. *Nanoscale* **2016**, *8* (41), 17947-17952.

(56) Badr, O.; Probert, S. Sinks and environmental impacts for atmospheric carbon monoxide. Appl. Energy **1995**, *50* (4), 339-372.

(57) Wetterskog, E.; Agthe, M.; Mayence, A.; Grins, J.; Wang, D.; Rana, S.; Ahniyaz, A.; Salazar-Alvarez, G.; Bergström, L. Precise control over shape and size of iron oxide nanocrystals suitable for assembly into ordered particle arrays. *Sci. Technol. Adv. Mater.* **2014**, *15* (5), 055010.

(58) Pénicaud, C.; Monclus, V.; Perret, B.; Passot, S.; Fonseca, F. Life cycle assessment of the production of stabilized lactic acid bacteria for the environmentally-friendly preservation of living cells. *J. Clean. Prod.* **2018**, *184*, 847-858.

(59) Faivre, D.; Menguy, N.; Pósfai, M.; Schüler, D. Environmental parameters affect the physical properties of fast-growing magnetosomes. *Am. Mineral.* **2008**, *93* (2-3), 463-469.

(60) Ali, I.; Peng, C.; Khan, Z. M.; Naz, I. Yield cultivation of magnetotactic bacteria and magnetosomes: a review. *J. Basic Microbiol.* **2017**, *57* (8), 643-652.

(61) Amelio, A.; Genduso, G.; Vreysen, S.; Luis, P.; Van der Bruggen, B. Guidelines based on life cycle assessment for solvent selection during the process design and evaluation of treatment alternatives. Green Chem. **2014**, *16* (6), 3045-3063.

(62) Joshi, D. R.; Adhikari, N. An overview on common organic solvents and their toxicity. *J. Pharm. Res. Int.* **2019**, 1-18.

(63) Tobiszewski, M.; Namieśnik, J. Pena-Pereira, F. Environmental risk-based ranking of solvents using the combination of a multimedia model and multi-criteria decision analysis. *Green Chem.* **2017**, *19* (4), 1034-1042.

(64) Wang, Y.; Maksimuk, S.; Shen, R.; Yang, H. Synthesis of iron oxide nanoparticles using a freshly-made or recycled imidazolium-based ionic liquid. *Green Chem.* **2007**, *9* (10), 1051-1056.

(65) Tobiszewski, M.; Namieśnik, J. Greener organic solvents in analytical chemistry. Curr. Opin. Green Sustain. Chem. **2017**, *5*, 1-4.

(66) Zhang, Y.; Bakshi, B. R. Demessie, E. S., Life cycle assessment of an ionic liquid versus molecular solvents and their applications. *Environ. Sci. Technol.* **2008**, *42* (5), 1724-1730.

(67) Huijbregts, M. A.; Hellweg, S.; Frischknecht, R.; Hendriks, H. W.; Hungerbuhler, K.; Hendriks, A. J. Cumulative energy demand as predictor for the environmental burden of commodity production. *Environ. Sci. Technol.* **2010**, *44* (6), 2189-2196.

(68) Huijbregts, M. A. J.; Rombouts, L. J. A.; Hellweg, S.; Frischknecht, R.; Hendriks, A. J.; Van de Meent, D.; Ragas, A. M. J.; Reijnders, L.; Struijs, J. Is cumulative fossil energy demand a useful indicator for the environmental performance of products? *Environ. Sci. Technol.* **2006**, *40*, 641–648.

(69) Sadhukhan, J.; Joshi, N.; Shemfe, M.; Lloyd, J. R. Life cycle assessment of sustainable raw material acquisition for functional magnetite bionanoparticle production. *J. Environ. Manag.* **2017**, *199*, 116-125.

(70) Blakemore, R.; Frankel, R., *Iron biominerals*: Springer Science & Business Media, 2013.

(71) Baumgartner, J.; Morin, G.; Menguy, N.; Gonzalez, T. P.; Widdrat, M.; Cosmidis, J.; Faivre, D. Magnetotactic bacteria form magnetite from a phosphate-rich ferric hydroxide via nanometric ferric (oxyhydr) oxide intermediates. *Proc. Natl. Acad. Sci. U. S. A.* **2013**, *110* (37), 14883-14888.

(72) Temizel-Sekeryan, S.; Hicks, A. L., Global environmental impacts of silver nanoparticle production methods supported by life cycle assessment. *Resour. Conserv. Recycl*. **2020**, *156*, 104676.

(73) Temizel-Sekeryan, S.; Hicks, A. L., Cradle-to-grave environmental impact assessment of silver enabled t-shirts: Do nano-specific impacts exceed non nano-specific emissions? *NanoImpact* **2021**, *22*, 100319.